



# Interplay between Asters/GRAMD1s and phosphatidylserine in intermembrane transport of LDL cholesterol

Michael N. Trinh<sup>a,1</sup>, Michael S. Brown<sup>a,2</sup>, Joachim Seemann<sup>b</sup>, Gonçalo Vale<sup>a,c</sup>, Jeffrey G. McDonald<sup>a,c</sup>, Joseph L. Goldstein<sup>a,2</sup>, and Feiran Lu<sup>a,1</sup>

<sup>a</sup>Department of Molecular Genetics, University of Texas Southwestern Medical Center, Dallas, TX 75390; <sup>b</sup>Department of Cell Biology, University of Texas Southwestern Medical Center, Dallas, TX 75390; and <sup>c</sup>Center for Human Nutrition, University of Texas Southwestern Medical Center, Dallas, TX 75390

Contributed by Joseph L. Goldstein; received November 8, 2021; accepted December 1, 2021; reviewed by Peter Tontonoz and Jean Vance

**Low-density lipoprotein (LDL) delivers cholesterol to mammalian cells through receptor-mediated endocytosis. The LDL cholesterol is liberated in lysosomes and transported to the plasma membrane (PM) and from there to the endoplasmic reticulum (ER). Excess ER cholesterol is esterified with a fatty acid for storage as cholesteryl esters. Recently, we showed that PM-to-ER transport of LDL cholesterol requires phosphatidylserine (PS). Others showed that PM-to-ER transport of cholesterol derived from other sources requires Asters (also called GRAMD1s), a family of three ER proteins that bridge between the ER and PM by binding to PS. Here, we use a cholesterol esterification assay and other measures of ER cholesterol delivery to demonstrate that Asters participate in PM-to-ER transport of LDL cholesterol in Chinese hamster ovary cells. Knockout of the gene encoding PTDSS1, the major PS-synthesizing enzyme, lowered LDL-stimulated cholesterol esterification by 85%, whereas knockout of all three Aster genes lowered esterification by 65%. The reduction was even greater (94%) when the genes encoding PTDSS1 and the three Asters were knocked out simultaneously. We conclude that Asters participate in LDL cholesterol delivery from PM to ER, and their action depends in large part, but not exclusively, on PS. The data also indicate that PS participates in another delivery pathway, so far undefined, that is independent of Asters.**

cholesterol | plasma membrane | Aster/GRAMD1 proteins | phosphatidylserine | mammalian cells

Animal cells obtain cholesterol through the receptor-mediated endocytosis of cholesterol-carrying plasma low-density lipoprotein (LDL) (1). The LDL particle is digested in lysosomes and the liberated cholesterol is transported to the plasma membrane (PM), where it fills three pools: 1) an accessible pool that is available to bind bacterial cytolysins such as perfringolysin O; 2) a sequestered pool that is bound to sphingomyelin; and 3) an essential pool whose depletion leads to cell death (2–4). Once the three pools have been filled, excess cholesterol is transported from the PM to the endoplasmic reticulum (ER), where it inhibits the proteolytic activation of sterol regulatory element-binding protein-2 (SREBP-2), a transcription factor that activates genes encoding the LDL receptor and enzymes of cholesterol synthesis (5). This inhibition lowers the uptake and synthesis of cholesterol, preventing excess accumulation. Any excess ER cholesterol is detoxified by acyl-CoA:cholesterol acyltransferase (ACAT), which esterifies cholesterol with a long-chain fatty acid such as oleate and incorporates it into lipid droplets for storage (1, 6).

Recently, several mechanisms underlying the nonvesicular movement of cholesterol between membranes have been elucidated (reviewed in ref. 7). Elegant work from the laboratories of Tontonoz and coworkers (8, 9) and Saheki and coworkers (10, 11) defined the role of membrane proteins named GRAMD1s or Asters in the transport of cholesterol from the PM to the ER. For simplicity, we use the term Aster.

Mammalian cells express three Asters, designated A, B, and C. Asters are anchored in the ER membrane by virtue of a membrane-spanning helix near the carboxy terminus. The cytosolic amino-terminal region contains two functional domains: a GRAM domain that binds anionic lipids and a START-like domain that binds cholesterol. When the accessible pool of PM cholesterol expands, the GRAM domain is triggered to bind to the PM, creating a bridge between the ER and the PM. Binding is postulated to be triggered by the known ability of the GRAM domain to bind anionic phospholipids, including phosphatidylserine (PS), that inhabit the inner leaflet of the PM. Binding to the PM has been demonstrated in vivo by total internal reflection fluorescence (TIRF) microscopy using EGFP-tagged GRAMD1s (10, 11) or Asters (8, 9). Binding is triggered when the accessible pool of PM cholesterol is increased by incubation with cholesterol/cyclodextrin complexes (8, 11) or by treatment with sphingomyelinase (10, 11), which expands the accessible pool by releasing cholesterol from the sequestered pool (2).

Our laboratory has focused on cholesterol movement from the accessible pool in the PM to the ER, a key step that allows the ER to monitor and optimize the level of PM cholesterol

## Significance

**Cholesterol constitutes 50% of lipids in the plasma membrane (PM) of animal cells. Sensors in the endoplasmic reticulum (ER) maintain this level by adjusting cholesterol uptake, synthesis, and storage. Uptake is mediated by LDL receptors, which deliver cholesterol-carrying LDL to lysosomes from which cholesterol moves to the PM and then to the ER. We report PM-to-ER transport of LDL cholesterol requires cholesterol-binding Aster proteins anchored to the ER and phosphatidylserine embedded in the PM. Asters are known to bind phosphatidylserine, and this accounts for part of the phosphatidylserine requirement. However, the current data suggest an additional requirement for phosphatidylserine independent of Asters. These data advance our knowledge of PM cholesterol homeostasis, a control mechanism essential for cell growth and survival.**

Author contributions: M.N.T., M.S.B., J.L.G., and F.L. designed research; M.N.T., J.S., G.V., J.G.M., and F.L. performed research; M.N.T., M.S.B., J.S., G.V., J.G.M., J.L.G., and F.L. analyzed data; and M.N.T., M.S.B., J.L.G., and F.L. wrote the paper.

Reviewers: P.T., University of California, Los Angeles; and J.V., University of Alberta.

The authors declare no competing interest.

This open access article is distributed under [Creative Commons Attribution-NonCommercial-NoDerivatives License 4.0 \(CC BY-NC-ND\)](https://creativecommons.org/licenses/by-nc-nd/4.0/).

<sup>1</sup>M.N.T. and F.L. contributed equally to this work.

<sup>2</sup>To whom correspondence may be addressed. Email: [mike.brown@utsouthwestern.edu](mailto:mike.brown@utsouthwestern.edu) or [joe.goldstein@utsouthwestern.edu](mailto:joe.goldstein@utsouthwestern.edu).

This article contains supporting information online at <http://www.pnas.org/lookup/suppl/doi:10.1073/pnas.2120411119/-DCSupplemental>.

Published January 6, 2022.

(3). In this context, we recently discovered another requirement for PM-to-ER cholesterol transport, namely PS (12). We conducted a CRISPR-Cas9 knockout screen for genes required for transport of LDL cholesterol from the lysosome to the ER. The screen disclosed a requirement for PTDSS1, the major PS-synthesizing enzyme in mammalian cells (13). PS is reduced by 90% in human cells lacking PTDSS1 (12). When LDL is added to these cells, the particle is taken up and digested in lysosomes normally, and the LDL-derived cholesterol reaches the PM, but in the absence of PS the cholesterol fails to move from the PM to the ER. As a result, the accessible pool of cholesterol in the PM increases, cleavage of SREBP-2 is not suppressed normally, and excess cholesterol is not esterified. All of these deficits are reversed when PS is restored by incubating the *Ptdss1*<sup>-/-</sup> cells with PS liposomes. We hypothesized that the cholesterol transport defect in the PS-deficient cells results from the failure of Asters to transport cholesterol (12).

In the current study, we have tested this hypothesis by preparing hamster cells that lack all three Asters with or without PTDSS1. The results indicate that loss of Aster function accounts for some, but not all of the block in cholesterol transport in PS-deficient cells. The data also suggest the existence of a second PS-dependent pathway that is independent of Asters. This paper explores the interplay between these two pathways.

## Results

The current experiments were performed with a line of Chinese hamster ovary (CHO) cells designated CHO-K1. Fig. 1A shows that CHO-K1 cells express mRNAs encoding all three Aster isoforms, with Aster-A expression being the highest. When we used CRISPR-Cas9 to knock out the *Gramd1a* gene encoding Aster-A, the mRNA for Aster-B increased (Fig. 1A). Therefore, to eliminate all Aster expression, we performed serial transfections with CRISPR-Cas9 plasmids to inactivate both copies of all three *Gramd1* genes (SI Appendix, Fig. S1). The resulting cells, designated *Aster-abc*<sup>-/-</sup>, did not express significant amounts of any of the Aster mRNAs (Fig. 1A). We also used CRISPR-Cas9 to eliminate the gene encoding PTDSS1, the enzyme that synthesizes PS. Fig. 1A shows that Aster-A and -B expression increased approximately twofold in the *Ptdss1*<sup>-/-</sup> cells.

The *Aster-abc*<sup>-/-</sup> cells and *Ptdss1*<sup>-/-</sup> cells exhibited normal uptake of LDL labeled with BODIPY-FL, a fluorescent lipid that integrates into the hydrophobic core of LDL (Fig. 1B). Uptake was blocked by an excess of unlabeled LDL, confirming that it was mediated by a saturable receptor. Indeed, uptake was absent in cells lacking the gene encoding the LDL receptor (Fig. 1B). We used two assays to measure the delivery of LDL cholesterol to the ER. One assay measures cholesterol esterification, and the other measures inhibition of the proteolytic processing of SREBP-2. Despite the normal uptake of LDL, the *Aster-abc*<sup>-/-</sup> cells and the *Ptdss1*<sup>-/-</sup> cells showed major deficits in the incorporation of [<sup>14</sup>C]oleate into cholesteryl esters (Fig. 1C). In wild-type (WT) cells, LDL inhibited the proteolytic processing of SREBP-2 by 82%, as reflected by a reduction in the ratio between the nuclear fragment and the membrane-bound precursor observed on SDS-PAGE (Fig. 1D). Inhibition by LDL was decreased in the *Aster-abc*<sup>-/-</sup> cells (<59%), and it was even less in the *Ptdss1*<sup>-/-</sup> cells (14%).

As shown previously for human cells (12), the level of PS was reduced by 90% in CHO-K1 cells lacking PTDSS1 (SI Appendix, Fig. S2). The level of phosphatidylethanolamine (PE) was also reduced since PE is formed from PS (13). In the previous studies, we also showed that addition of PS overcomes the block in cholesterol transport in human *Ptdss1*<sup>-/-</sup> cells (12). To determine whether PS would overcome the block in the hamster *Aster-abc*<sup>-/-</sup> cells, we incubated the cells with

cholesterol complexed to methyl- $\beta$ -cyclodextrin (MCD), which delivers cholesterol directly to the PM (14). To measure cholesterol delivery to the ER, we used the cholesterol esterification assay. In WT cells, addition of cholesterol/MCD led to an increase in the incorporation of [<sup>14</sup>C]oleate into cholesteryl esters, and addition of PS caused a slight further increase (Fig. 2A). In the *Ptdss1*<sup>-/-</sup> cells, cholesterol esterification was low and was restored nearly to normal with PS supplementation (Fig. 2B). Cholesterol esterification was also low in the *Aster-abc*<sup>-/-</sup> cells, and there was no restoration by PS (Fig. 2C). We also produced cells lacking all three Asters as well as PTDSS1 (SI Appendix, Fig. S1). In these cells cholesterol was not esterified, and there was a slight but consistent increase when PS was added (Fig. 2D).

In the same experiment, we also used human LDL to deliver cholesterol to the CHO-K1 cells (Fig. 2E-H). Whereas MCD delivers cholesterol directly to the PM, LDL delivers cholesterol to the lysosome, from which it is transported to the PM. When LDL was added, the results of the cholesterol esterification assay were directionally similar to the ones obtained with cholesterol/MCD, but the absolute amount of esterification was lower. In WT cells, LDL cholesterol reached the ER where it was esterified with [<sup>14</sup>C]oleate, and the addition of PS had no effect (Fig. 2E). Esterification was reduced in the *Ptdss1*<sup>-/-</sup> cells and was restored with PS addition (Fig. 2F). Esterification was reduced in the *Aster-abc*<sup>-/-</sup> cells and was not restored by PS (Fig. 2G). Esterification was even lower in the *Ptdss1*<sup>-/-</sup>; *Aster-abc*<sup>-/-</sup> cells, and there was a small but consistent increase when PS was added.

Fig. 2I and J present the cholesterol esterification rates observed in five independent studies in which duplicate dishes from WT or mutant CHO-K1 cells were treated with cholesterol/MCD at 300  $\mu$ M (Fig. 2I) or 100  $\mu$ g/mL LDL (Fig. 2J). The results from each of the 10 dishes are expressed as a percentage of the esterification observed in WT cells on the same day. Independently of whether cholesterol was added in complex with MCD or contained in LDL, cholesterol esterification in *Ptdss1*<sup>-/-</sup>; *Aster-abc*<sup>-/-</sup> cells was lower than the rate in either *Ptdss1*<sup>-/-</sup> cells or the *Aster-abc*<sup>-/-</sup> cells. This observation indicates that the PS-dependent pathway and the Aster-dependent pathway are partially independent (Discussion).

In the experiment of Fig. 3A, we incubated cells with LDL and measured the relative amount of cholesterol in the PM by incubating the cells with AF488-PFO\*, a fluorescently tagged, genetically optimized form of bacterial perfringolysin O that binds to accessible cholesterol in PMs (12, 15). AF488-PFO\* binding was quantitated by flow cytometry (Fig. 3A), and the median cellular fluorescence was calculated (Fig. 3B). As we previously reported (12), after incubation with LDL, *Ptdss1*<sup>-/-</sup> cells showed an increase in PM cholesterol as reflected by increased AF488-PFO\* binding. A similar increase was observed in the *Aster-abc*<sup>-/-</sup> cells (Fig. 3A and B). The increase was greater when the two deficits were combined in the *Ptdss1*<sup>-/-</sup>; *Aster-abc*<sup>-/-</sup> cells. We also stained the cells with AF488-PFO\* while grown on coverslips (Fig. 3C). Staining of the PM was increased in the *Ptdss1*<sup>-/-</sup> cells and in the *Aster-abc*<sup>-/-</sup> cells, and the intensity was increased further in the *Ptdss1*<sup>-/-</sup>; *Aster-abc*<sup>-/-</sup> cells. Sequestration of LDL-derived cholesterol in the PM led to a decrease in cholesterol esterification in the *Aster-abc*<sup>-/-</sup> cells and in the *Ptdss1*<sup>-/-</sup> cells (Fig. 3D). The decrease was even greater in the *Ptdss1*<sup>-/-</sup>; *Aster-abc*<sup>-/-</sup> cells, consistent with the greater trapping of LDL cholesterol in the PM.

The data thus far indicate that Asters and PS are both required for maximal transport of cholesterol from the PM to the ER. To further explore the relation between the two requirements, we incubated cells with varying concentrations of cholesterol/MCD and used the cholesterol esterification assay

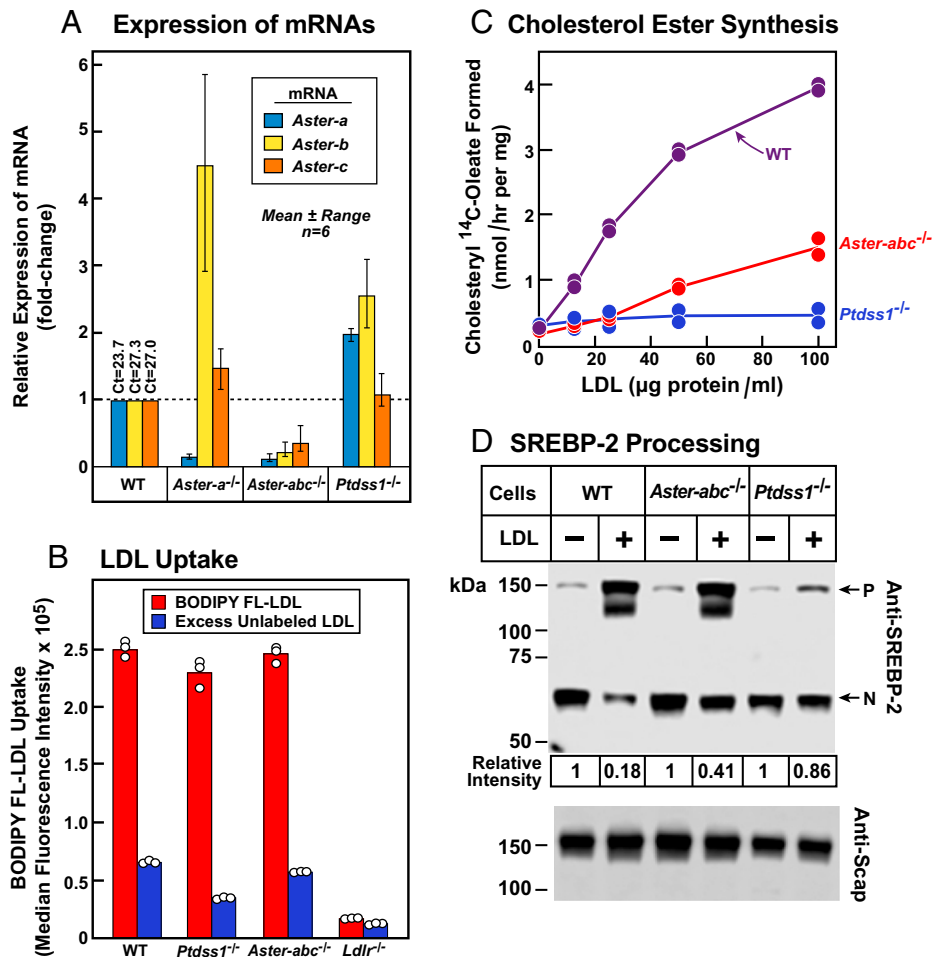


**Fig. 1.** Asters and PTSS1 required for delivery of LDL cholesterol to the ER in CHO-K1 cells. All cells were set up on day 0 in medium A with 10% fetal calf serum (FCS). (A) mRNA expression of Aster-A, -B, and -C in WT and mutant cell lines. On day 2, cells were switched to cholesterol-depletion medium A. After incubation for 16 h, cells received cholesterol-depletion medium B containing 50 µg protein/mL human LDL. After 6 h, cells were harvested for RNA extraction and quantitative RT-PCR as described in *SI Appendix, Materials and Methods*.  $C_t$  values for expression of *Aster-a*, *-b*, and *-c* in WT cells are shown. The mRNA levels for *Aster-a*, *-b*, and *-c* in the mutant cell lines are expressed relative to the  $C_t$  values in the WT cells. Mean and range of six replicates are shown. (B) BODIPY FL-LDL uptake. On day 2, cells were switched to cholesterol-depletion medium A. After incubation for 16 h, cells received cholesterol-depletion medium B containing 5 µg protein/mL BODIPY FL-LDL in absence (red) or presence (blue) of 150 µg protein/mL of unlabeled human LDL. After 6 h, cells were harvested for flow cytometry. The heights of the bars indicate the mean of triplicate incubations. (C) Stimulation of cholesteryl ester synthesis by LDL in WT, *Aster-abc*<sup>-/-</sup>, and *Ptdss1*<sup>-/-</sup> cells. On day 2, cells were refed with cholesterol-depletion medium A. After incubation for 16 h, cells received cholesterol-depletion medium B containing the indicated amount of LDL. After 4 h, cells were pulse labeled for 2 h with 0.1 mM sodium [<sup>14</sup>C]oleate (7,157 dpm/nmol), after which the cellular content of cholesteryl [<sup>14</sup>C]oleate was measured. The lines denote the average of duplicate incubations with individual values shown. (D) SREBP-2 processing. On day 2, cells were switched to cholesterol-depletion medium A containing 1% hydroxypropyl-β-cyclodextrin (HPCD). After incubation for 1 h, the cells received cholesterol-depletion medium A in absence or presence of 100 µg protein/mL LDL. After 6 h, cells were harvested for extraction, SDS-PAGE, and immunoblotting of SREBP-2 and Scap (*SI Appendix, Materials and Methods*). P, precursor. N, nuclear. SREBP cleavage was quantified using ImageJ (16). For each lane, the ratio of nuclear to total SREBP-2 (i.e., nuclear + precursor) was calculated and expressed relative to the value in WT cells without LDL.

to monitor delivery of cholesterol to the ER (Fig. 4). At high levels of cholesterol/MCD (300 and 500 µM cholesterol), esterification was reduced equally in the *Aster-abc*<sup>-/-</sup> and *Ptdss1*<sup>-/-</sup> cells (Fig. 4A). Esterification was reduced much further in the cells lacking both PTSS1 and Asters, indicating that PS and Asters participate in two pathways that are partially independent and necessary for maximal transport (*Discussion*). The situation was different at low levels of PM cholesterol, as illustrated by the expanded graph in Fig. 4B. At cholesterol/MCD concentrations between 25 and 100 µM, esterification in the *Aster-abc*<sup>-/-</sup> cells was much lower than in the *Ptdss1*<sup>-/-</sup> cells, which retain their Aster proteins. These data indicate that at low PM-cholesterol concentrations, the delivery of cholesterol to the ER is more dependent on the Asters than on the PS pathway. Stated differently, when cholesterol is added with

MCD, the Aster pathway appears to have a higher affinity for PM cholesterol than does the PS-dependent pathway.

## Discussion

Previous studies from the laboratories of Tontonoz and coworkers (8, 9) and Saheki and coworkers (10, 11) demonstrated that Aster proteins are required for the transport of cholesterol from the PM to the ER when cholesterol is delivered directly to the PM by incubation with cholesterol/MCD complexes or when it is liberated within the membrane by sphingomyelinase treatment. Our previous study showed that PS is required for PM-to-ER cholesterol transport when cholesterol is delivered to the cell by LDL or cholesterol/MCD (12). Inasmuch as Asters are known to bind to negatively charged phospholipids,

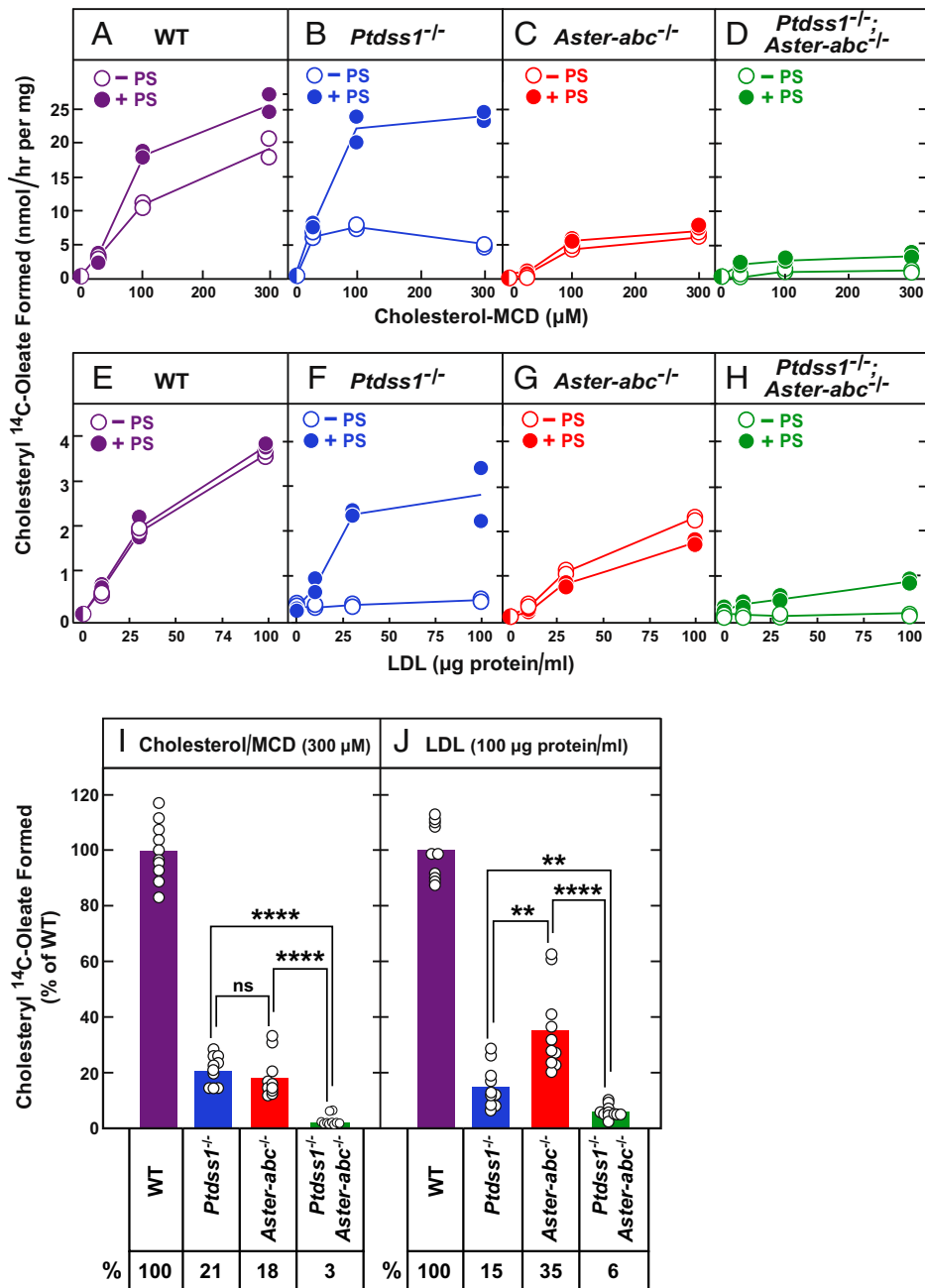


**Fig. 2.** (A–H) PS corrects block in cholesterol transport in *Ptdss1*<sup>-/-</sup> cells, but not in *Aster-abc*<sup>-/-</sup> cells. On day 0, WT and mutant CHO-K1 cells were set up in medium A with 10% FCS. On day 2, cells were refed with cholesterol-depletion medium A in the absence or presence of 10 μM PS liposomes. After incubation for 16 h, cells received cholesterol-depletion medium B and the indicated amount of cholesterol/MCD (A–D) or LDL (E–H) in the absence or presence of 10 μM PS liposomes. After 4 h, cells were pulse labeled for 2 h with 0.1 mM sodium [<sup>14</sup>C]oleate (7,988 dpm/nmol), after which the cellular content of cholesteryl [<sup>14</sup>C]oleate was measured. The lines denote the average of duplicate incubations with individual values shown. (I and J) Relative rate of cholesterol esterification in WT and mutant CHO-K1 cells incubated with cholesterol/MCD or LDL. Cells were set up as described above. Each bar shows the values from five independent experiments in which duplicate dishes of cells were incubated for 3 or 4 h with either 300 μM cholesterol/MCD (I) or 100 μg protein/mL LDL (J) and pulsed for 2 h with 0.1 mM [<sup>14</sup>C]oleate (7,091 to 10,591 dpm/nmol) as described above. Each value in the mutant cells is expressed relative to the esterification rate in WT cells in the same experiment. Statistical analysis was performed using Student's *t* test. ns, no significance; \*\**P* < 0.01, \*\*\*\**P* < 0.0001.

including PS, we hypothesized that the role of PS is to support Aster function. In the current study, we tested this hypothesis using genetically modified Chinese hamster cells. The data demonstrate that: 1) Aster proteins are indeed required for normal rates of PM-to-ER transport of LDL-derived cholesterol after it moves from lysosomes to the PM; 2) Aster-mediated transport is dependent on PS, but only partially; and

3) in addition to supporting Aster-mediated transport, PS is required for another PM-to-ER cholesterol transport pathway that is independent of Asters.

The requirement for Asters in transport of LDL-derived cholesterol from the PM to the ER is revealed by the data in Figs. 1–3. LDL uptake in the *Aster-abc*<sup>-/-</sup> cells was the same as in WT cells (Fig. 1B), but the rate of cholesterol ester synthesis

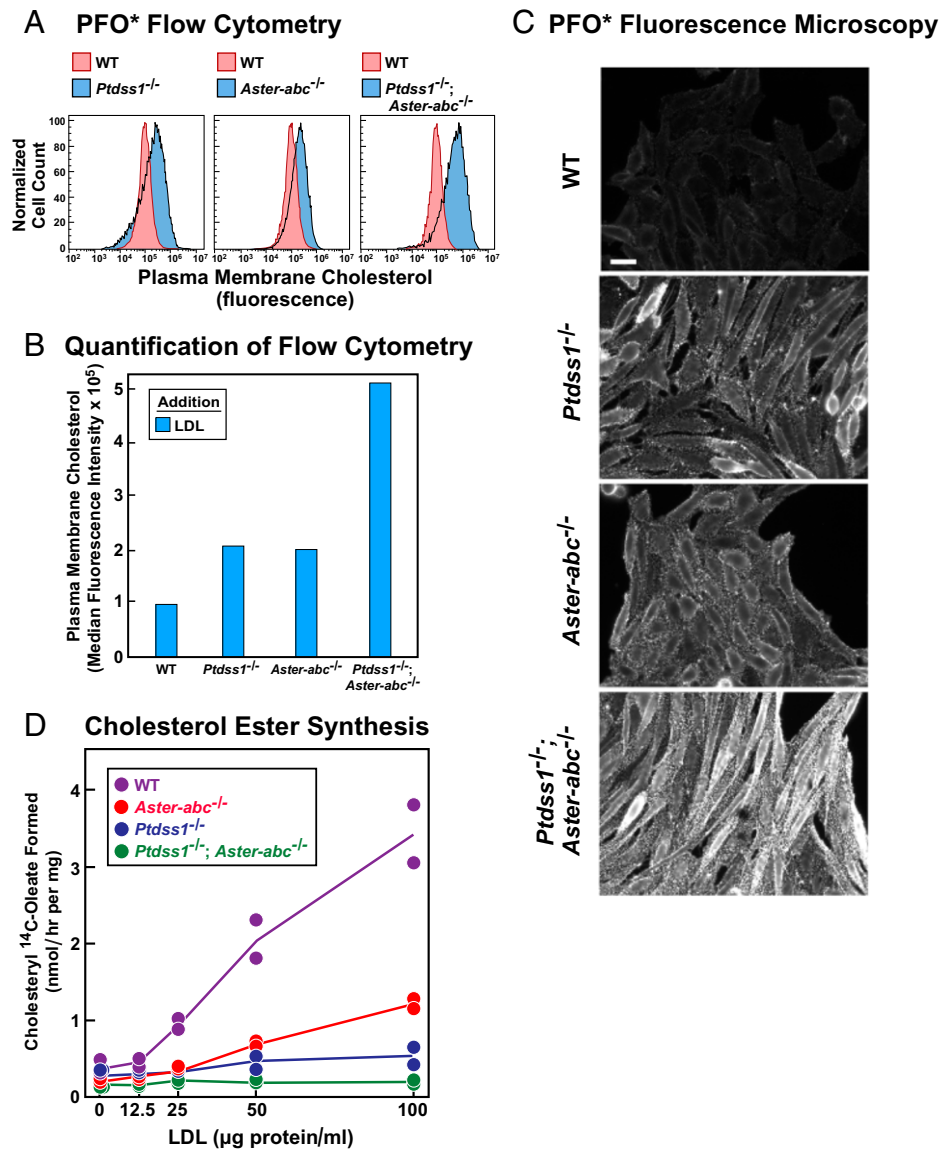


**Fig. 3.** LDL-derived cholesterol accumulates in the PM of *Ptdss1<sup>-/-</sup>* and *Aster-abc<sup>-/-</sup>* cells. (A) Measurement of PM cholesterol by flow cytometry. On day 0, the indicated WT and mutant cells were set up in medium A with 10% FCS. On day 2, cells were switched to cholesterol-depletion medium A. After incubation for 16 h, cells received cholesterol-depletion medium B containing the indicated concentration of LDL. After 6 h, cells were incubated with AF488-labeled PFO\* and subjected to flow cytometry as described in *SI Appendix, Materials and Methods*. For comparison, the same WT control histogram is shown in all panels. (B) Median fluorescence intensity values in A were calculated as described in *SI Appendix, Materials and Methods*. (C) Visualization of PM cholesterol. On day 0, the indicated cells were plated in six-well plates containing 12-mm glass coverslips in medium A with 10% FCS. On day 3, AF488-conjugated-PFO\* was added and cells were imaged as described in *SI Appendix, Materials and Methods*. (Scale bar, 20 μm.) (D) Stimulation of cholesteryl ester synthesis by LDL. On day 0, cells were set up in medium A with 10% FCS. On day 2, cells were refed with cholesterol-depletion medium A. After incubation for 16 h, cells received cholesterol-depletion medium B and the indicated amount of LDL. After 4 h, cells were pulse labeled for 2 h with 0.1 mM sodium [<sup>14</sup>C]oleate (8,500 dpm/nmol), after which cellular content of cholesteryl [<sup>14</sup>C]oleate was measured. Each line denotes the average of duplicate incubations with individual values shown.

was less (see the individual experiments in Figs. 1–3 and the averaged data from five experiments in Fig. 2J). Moreover, LDL did not inhibit SREBP-2 processing as much in the *Aster-abc<sup>-/-</sup>* cells as it did in WT cells (Fig. 1D). Instead of reaching the ER in normal amounts, in the *Aster-abc<sup>-/-</sup>* cells LDL-derived cholesterol accumulated in the PM as it did in *Ptdss1<sup>-/-</sup>* cells (Fig. 3 A–C). Finally, addition of PS liposomes restored transport of LDL-derived cholesterol nearly to normal in the *Ptdss1<sup>-/-</sup>* cells (Fig. 2F), but the restoration was much less when the *Ptdss1<sup>-/-</sup>* cells also lacked Asters (Fig. 2H). Considered together, all of these data indicate that Aster proteins and PS

are both required for transport of LDL-derived cholesterol from the PM to the ER in CHO-K1 cells.

Although PS and Asters are both required for normal PM-to-ER cholesterol transport, their functions overlap only partially. This conclusion is based on a genetic epistasis analysis. If Aster proteins absolutely require PS for function, then the *Ptdss1<sup>-/-</sup>* cells should lack Aster function, and the addition of Aster deficiency in the *Ptdss1<sup>-/-</sup>; Aster-abc<sup>-/-</sup>* cells should produce no further reduction. However, this was not the case. As shown in Fig. 2 I and J, cholesterol esterification in the *Ptdss1<sup>-/-</sup>; Aster-abc<sup>-/-</sup>* cells was significantly lower than in the *Ptdss1<sup>-/-</sup>* cells whether

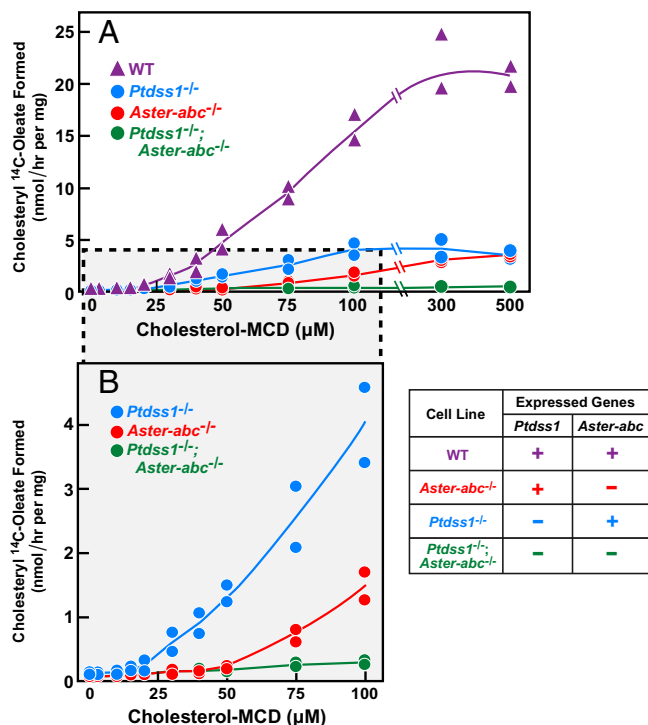


**Fig. 4.** Asters mediate high-affinity transport of cholesterol derived from cholesterol/MCD. (A) On day 0, the indicated cells were set up in medium A with 10% FCS. On day 2, cells were refed with cholesterol-depletion medium A. After incubation for 16 h, cells received cholesterol-depletion medium B containing the indicated amount of cholesterol/MCD. After 3 h, cells were pulse labeled for 2 h with 0.1 mM sodium [<sup>14</sup>C]oleate (9,750 dpm/nmol), after which the cellular content of cholesteryl [<sup>14</sup>C]oleate was measured. Lines denote the mean of duplicate incubations with individual values shown. (B) An expanded version of the data in A, highlighting the values for cholesterol/MCD at concentrations below 100 μM. Similar results were obtained when this experiment was repeated on 3 different days.

cholesterol was introduced with MCD (Fig. 2I) or with LDL (Fig. 2J). This finding indicates that Aster proteins must have contributed to transport in the *Ptdss1*<sup>-/-</sup> cells despite the 90% reduction in PS (SI Appendix, Fig. S2B). We cannot exclude the possibility that the Aster function in the *Ptdss1*<sup>-/-</sup> cells is attributable to the 10% of PS that is retained in those cells. However, the known ability of Asters to bind to other anionic lipids suggests that one or more of these lipids may be able to maintain some Aster function when PS is severely deficient.

The epistasis analysis also indicates that PS is required for a transport process that is independent of Asters. If PS were required only to support Aster function, then the *Aster-abc*<sup>-/-</sup> cells should lack all functions of PS, and the addition of PTDSS1 deficiency should produce no further reduction. Again this was not the case. As shown in Fig. 2I and J, adding PTDSS1 deficiency to Aster deficiency caused a further reduction in cholesterol esterification, indicating that, in addition to supporting Aster function, PTDSS1 is required for another PM-to-ER cholesterol transport process that is independent of Asters.

Further evidence for the role of PS in Aster function is illustrated by the *Upper* panels in Fig. 2. As we showed previously (12), restoration of cellular PS by addition of PS-containing liposomes restored cholesterol delivery from the PM to the ER in *Ptdss1*<sup>-/-</sup> cells, as manifested by an increase in cholesterol esterification after addition of cholesterol/MCD (Fig. 2B). Similar restoration occurred when cholesterol was delivered in LDL (Fig. 2F). Restoration was much less when the *Ptdss1*<sup>-/-</sup> cells lacked Asters (Fig. 2D and H).

The current data raise two questions for future study of PM-to-ER cholesterol transport. First, what is the substance that can support partial Aster function in the absence of PS? It is likely to be another negatively charged lipid, perhaps phosphatidylinositol, which is already known to bind to Asters (11). Second, what is the Aster-independent pathway that requires PS? Does it depend on contact sites between the PM and the ER or could it involve a vesicular mechanism through endocytosis of cholesterol-rich membranes? These questions should be answered now that the roles of Asters and PS have been distinguished.

## Materials and Methods

Reagents, mutant cell lines and knockouts, plasmids, purification and labeling of PFO\*, BODIPY FL-LDL uptake, PFO\* binding, visualization of PFO\* binding by fluorescence microscopy, flow cytometry, cholesteryl ester synthesis, PS unilamellar liposomes, SREBP-2 processing, immunoblot analysis, measurement of phospholipids by liquid chromatography with tandem mass spectrometry (LC-MS/MS), and reproducibility can be found in SI Appendix, Materials and Methods.

**Data Availability.** All study data are included in the article and/or SI Appendix.

**ACKNOWLEDGMENTS.** We thank our colleagues Jaeil Han, Joshua Mendell, and Marcel Mettlen for helpful discussions; Erin Ruhlman, Alexa Smith, and William Salter for excellent technical assistance; and Lisa Beatty and Alexandra Hatten for invaluable help with tissue culture. This research was supported by grants from the NIH (HL20948 and GM096070) and the Welch Foundation (I-1910). M.N.T. was supported by the NIH Medical Scientist Training Program (GM008014) and is a recipient of the Paul & Daisy Soros Fellowships for New Americans.

- M. S. Brown, J. L. Goldstein, A receptor-mediated pathway for cholesterol homeostasis. *Science* **232**, 34–47 (1986).
- A. Das, M. S. Brown, D. D. Anderson, J. L. Goldstein, A. Radhakrishnan, Three pools of plasma membrane cholesterol and their relation to cholesterol homeostasis. *eLife* **3**, e02882 (2014).
- R. E. Infante, A. Radhakrishnan, Continuous transport of a small fraction of plasma membrane cholesterol to endoplasmic reticulum regulates total cellular cholesterol. *eLife* **6**, e25466 (2017).
- Y. Lange, T. L. Steck, Active cholesterol 20 years on. *Traffic* **21**, 662–674 (2020).
- M. S. Brown, J. L. Goldstein, Cholesterol feedback: From Schoenheimer's bottle to Scap's MELADL. *J. Lipid Res.* **50** (suppl.), S15–S27 (2009).
- T. Y. Chang, C. C. Y. Chang, D. Cheng, Acyl-coenzyme A: Cholesterol acyltransferase. *Annu. Rev. Biochem.* **66**, 613–638 (1997).
- E. Ikonen, X. Zhou, Cholesterol transport between cellular membranes: A balancing act between interconnected lipid fluxes. *Dev. Cell* **56**, 1430–1436 (2021).
- J. Sandhu *et al.*, Aster proteins facilitate nonvesicular plasma membrane to ER cholesterol transport in mammalian cells. *Cell* **175**, 514–529.e20 (2018).
- A. Ferrari *et al.*, Aster proteins regulate the accessible cholesterol pool in the plasma membrane. *Mol. Cell. Biol.* **40**, e00255-20 (2020).
- T. Naito *et al.*, Movement of accessible plasma membrane cholesterol by the GRAMD1 lipid transfer protein complex. *eLife* **8**, e51401 (2019).
- B. Ercan, T. Naito, D. H. Z. Koh, D. Dharmawan, Y. Saheki, Molecular basis of accessible plasma membrane cholesterol recognition by the GRAM domain of GRAMD1b. *EMBO J.* **40**, e106524 (2021).
- M. N. Trinh *et al.*, Last step in the path of LDL cholesterol from lysosome to plasma membrane to ER is governed by phosphatidylserine. *Proc. Natl. Acad. Sci. U.S.A.* **117**, 18521–18529 (2020).
- J. E. Vance, G. Tasseva, Formation and function of phosphatidylserine and phosphatidylethanolamine in mammalian cells. *Biochim. Biophys. Acta* **1831**, 543–554 (2013).
- U. Klein, G. Gimpl, F. Fahrenholz, Alteration of the myometrial plasma membrane cholesterol content with beta-cyclodextrin modulates the binding affinity of the oxytocin receptor. *Biochemistry* **34**, 13784–13793 (1995).
- A. Das, J. L. Goldstein, D. D. Anderson, M. S. Brown, A. Radhakrishnan, Use of mutant <sup>125</sup>I-perfringolysin O to probe transport and organization of cholesterol in membranes of animal cells. *Proc. Natl. Acad. Sci. U.S.A.* **110**, 10580–10585 (2013).
- C. A. Schneider, W. S. Rasband, K. W. Eliceiri, NIH Image to ImageJ: 25 years of image analysis. *Nat. Methods* **9**, 671–675 (2012).